Electrowetting Measurements with Mercury Showing Mercury/Mica Interfacial Energy Depends on Charging

David A. Antelmi, Jason N. Connor,† and Roger G. Horn*
Ian Wark Research Institute, University of South Australia, Mawson Lakes S.A. 5095, Australia
Received: August 10, 2003; In Final Form: November 4, 2003

We demonstrate that the interfacial energy between mercury and mica is a function of charge on the mercury surface, decreasing with increasing positive charge. The contact angle of mercury on mica has been measured as a function of potential applied to the mercury, which forms the working electrode of a cell containing either KCl or NaF electrolyte solution. At high negative applied potentials, a stable aqueous film exists between the mercury and mica surface. As potential is made less negative, the film collapses and mercury partially wets the mica at a critical potential, close to the electrocapillary maximum. Upon increasing the potential further (making the Hg surface more and more positive), the contact angle measured within the mercury continually decreases. Electrowetting with mercury is not unexpected since its interfacial tension with the aqueous phase is known to be a function of applied potential. However, the observed decrease goes against the trend expected from the Young equation if only this effect is considered. To explain the data we must allow the mercury/mica interfacial tension also to vary with applied potential. This variation indicates that the mercury surface is positively charged by contact with mica, consistent with known contact electrification between these two materials. The inherent charges at the mercury interfaces with mica and electrolyte solution result in contact angle changes of some tens of degrees with a change in applied potential of half a volt, orders of magnitude less than the potentials required to effect comparable changes in other electrowetting systems.

Introduction

Contact angle measurements are frequently used to investigate changes in the interfacial energy between two phases by application of the Young equation

$$\gamma_{13} = \gamma_{12} + \gamma_{23}\cos\theta \tag{1}$$

where phase **1** has a flat surface and the contact angle θ is measured in fluid phase **2**, both immersed in another (background) fluid phase **3**. The most common cause of variations in interfacial energy (and contact angle) is adsorption of a surface-active species at an interface. It should be noted that in some situations adsorption occurs at two interfaces simultaneously, in which case two interfacial energies are coupled.[1] For example, a surfactant dissolved in a water drop on a solid surface could adsorb both at the solid/water and at the air/water interface.

Another factor that affects interfacial energy is surface charge. The interfacial tension between mercury and aqueous electrolyte solutions, for example, is known to vary when an electrical potential E is applied between the two phases. Classical experiments using electrocapillarity and dropping mercury electrode techniques have shown that the interfacial tension between mercury and simple electrolyte solutions has a maximum (427 mJ/m^2 in NaF) at a certain value of applied potential E_{ecm} (the subscript means electrocapillary maximum), and decreases for applied potentials on either side of this value.[2] The decrease corresponds to increasing surface charge on the mercury in contact with the electrolyte, whether positive or negative, and the mercury charge is zero at E_{ecm} (which for this reason is sometimes called the point of zero charge, PZC).[3] The gradient of the electrocapillary curve $\gamma(E)$ gives the surface charge density σ through the Lippmann equation

$$\frac{\partial\gamma}{\partial E} = -\sigma \tag{2}$$

Some of the early measurements demonstrating this effect were made by measuring the rise of mercury into a glass capillary and deriving the interfacial energy with the assumption that the contact angle of mercury against the capillary material was constant. As has been pointed out by Lawrence et al.,[4] this assumption may not be correct. Those authors suggested that the contact angle of mercury on glass may vary when an applied potential changes γ_{23} in eq 1, as is known to occur with mercury/water. This question provided one of the original motivations for the present work.

We are also interested in following up previous investigations of the effect of potential on interfacial energies between mercury and other nonconducting materials. For example, early work by Koltoff and Kahan[5] and by Frumkin and co-workers[6] noted a dependence on applied potential of the time taken for mercury drops to detach from a glass capillary immersed in electrolyte solution. Smolders[7] showed that mercury/hydrogen gas interfacial energy varies with the potential applied between mercury and a neighboring electrolyte solution. Nakamura et al.[8] demonstrated the same effect between mercury and air. In contrast, the measurements of Ivosevic and Zutic[9] on the variation with potential of contact angle between an oil drop and mercury under electrolyte solutions found no potential dependence of the mercury/oil interfacial energy.

* To whom correspondence should be addressed. E-mail: roger.horn@unisa.edu.au.
† Present address: Process Engineering and Light Metals Centre, Central Queensland University, Gladstone, Queensland 4680, Australia.

10.1021/jp036371u CCC: $27.50
Published on Web 12/20/2003

The above changes have been attributed to a potential-dependent spreading pressure, which represents a reduction in interfacial tension between two phases when a third phase, for example water, is present. Some authors have discussed spreading pressure explicitly[6,8] while others have discussed the effect in qualitative terms.[7,9] The same concept has also appeared in work describing variations of mercury contact angle with factors other than applied potential, e.g. humidity[10] or electrolyte concentration.[11] We will return to a more detailed discussion of spreading pressures after presenting the results of our measurements of contact angles of a mercury drop against mica in electrolyte solutions when a potential is applied between the mercury and electrolyte phases.

In the same way that earlier investigations have demonstrated concomitant energy variations at mercury interfaces with two other materials, our results show that not only the mercury/aqueous but also the mercury/mica interfacial energy varies with the applied potential. However, rather than invoking a spreading pressure to explain the variation at the mercury/third phase interface, we offer a different explanation, namely that there is electrical charge separation across this interface. Thus a Lippmann relation (eq 2) applies here as well as at the mercury/aqueous interface, and the results allow us to calculate the magnitude and sign of the charge in the mercury phase. The sign that we determine is consistent with the natural contact electrification between mercury and mica, and its magnitude is consistent with a simple mechanism that we propose for the charging behavior.

It is interesting to note that because mercury is a conductor, charges within it must be distributed in such a way that the entire phase has a uniform electrical potential. This means that the amounts of charge present at its interfaces with two different phases (water and mica) are not independent of each other. Furthermore, as a consequence of this and the Lippmann relations, the two interfacial energies are also not independent of each other. This may have consequences for electrocapillarity and dropping mercury electrode measurements, in which mercury inevitably contacts a solid as well as an electrolyte solution.

Our experiments represent an example of electrowetting, which has been a topic of recent interest due to its potential applications in microfluidic devices,[12] controllable capillary rise,[13] and variable focus liquid lenses.[14] A useful survey of the literature is included in a recent article by Quinn et al.[15] Some authors have demonstrated electrowetting on metallic surfaces[16−18] and discussed the relationship to electrocapillarity. Other recent electrowetting studies have investigated changes in contact angle of a drop of aqueous solution on an electrode that is insulated by an adsorbed organic layer[19] or a thin polymer film;[15,20−22] one has looked at a drop of decane immersed in aqueous solution.[23] The phenomenon is explained by the stored energy of a capacitor formed by the insulating film between the electrode and the aqueous phase.[20] Apart from this effect the interfacial energies are assumed to be independent of applied potential, at least until large potentials are applied and a saturation phenomenon is observed.[15,22]

In contrast, the contact angle change of mercury that we report here occurs precisely because the interfacial energy is a function of potential, not only at one but at two interfaces. Furthermore, the high surface charge on mercury at its interfaces with water, and especially with mica, results in an electrowetting effect that is much stronger than the effects seen in the aqueous systems described above. Both types of experiment produce changes in contact angle of several tens of degrees, but in the aqueous/insulated electrode systems this requires potentials of hundreds of volts, compared to a fraction of a volt required to produce comparable changes in the mercury contact angle.

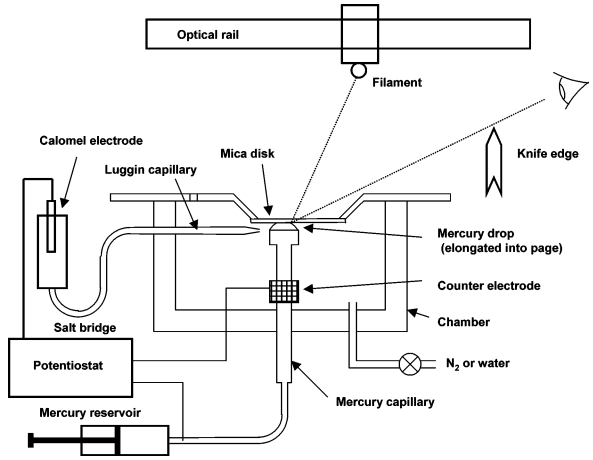

Figure 1. Apparatus for measuring the contact angle of mercury against a solid substrate, immersed in an electrolyte.

Experimental Section

Apparatus. The experimental apparatus developed to measure the mercury contact angle against a solid substrate is shown schematically in Figure 1. The apparatus consisted of a Kel-F chamber similar to that developed in our laboratory for interferometric measurements of thin film drainage and forces between mercury and a flat solid surface.[24,25] The chamber was covered with a stainless steel top plate that held a transparent solid against which the mercury could be contacted. The whole apparatus was mounted on adjustable supports so that the solid substrate could be leveled in the horizontal plane. Liquid mercury was held in a Teflon-lined stainless steel capillary that was fed through the bottom of the chamber. The capillary terminated in a rectangular trough (Kel-F) 3 mm wide × 8 mm long, in which the mercury formed an elongated droplet. The whole capillary tube could be moved up and down to engage or disengage the mercury drop and the solid surface. The reservoir of mercury was contained in two coupled syringes, one of 25 mL capacity and the other of 1 mL capacity, whose threaded plungers could be adjusted to give coarse or fine control of the mercury level protruding from the trough. In this way, when the mercury droplet was put into contact with the solid substrate, the advancing and receding angles could be carefully probed. Retracting the capillary far from the solid surface and spilling several drops of mercury out of the trough allowed the mercury drop surface to be renewed. This procedure was applied throughout the experiments to avoid the accumulation of contaminants on the mercury surface.

The solid substrate was a circular disk of freshly cleaved mica of diameter ∼40 mm. This was mounted in a rotating substrate holder fixed on the top plate. The axis of rotation of the substrate holder was offset with respect to the longitudinal axis of the mercury capillary so that rotating the mica disk in situ allowed fresh contact positions to be accessed.

Electrochemical Cell. The mercury droplet formed the working electrode of a three-electrode cell. A small piece of platinum wire, inserted through a Teflon septum at the opening of the larger syringe, made contact with the mercury allowing electrical connection to a potentiostat. The reference electrode (Ionode, Australia) was a calomel electrode saturated with KCl and the counter electrode was a platinum gauze cylinder of 15 mm diameter and 15 mm length. The mercury capillary ran

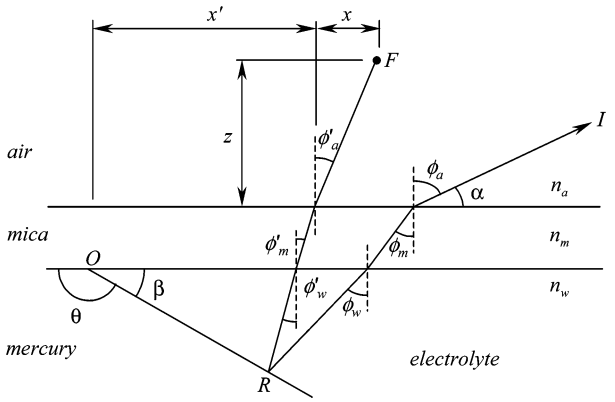

Figure 2. Geometry of the experiment (not to scale). Mercury makes the contact angle θ against the mica substrate at the three-phase line *O*. Rays from the filament pass through the mica substrate into the electrolyte and are reflected from the mercury surface. A reflected image occurs at a fixed point *I* depending on the contact angle θ and the location of the filament along *x*.

through the central axis of the counter electrode as shown in Figure 1. The potential applied to the mercury was controlled with use of a Wenking MP87 three-electrode potentiostat (Bank Elektronik, Germany).

Current between the working and counter electrodes was monitored throughout the experiments to keep check on the level of oxygen dissolved in the electrolyte. If significant current was detected, oxygen was purged from the solution by passing nitrogen gas through the apparatus. The N_2 gas was purified by passing it through an organic absorption medium followed by an oxygen-scrubbing coil (Alltech Oxy-Trap) prior to being introduced into the apparatus. The same gas was bubbled through the apparatus and electrolyte solutions before flooding the chamber.

Optical Setup. The contact angle in the mercury phase ($\theta > \pi/2$) was measured by using a reflective technique based on a method introduced by Langmuir and Schaeffer[26] and subsequently employed by other authors.[10,27] A small 6-V lamp was mounted on a movable carriage placed atop an optical rail above the apparatus. By monitoring the mercury surface at a point near the three-phase contact line, which is a straight line in the central region of the elongated drop, the reflected image of the filament could be seen as a bright spot at the appropriate viewing angle. The viewpoint on the mercury surface was observed at a fixed angle, set by glancing over a knife-edge rigidly fixed with respect to the apparatus (see Figure 1). By moving the filament along the rail, the angle of incidence changes and the filament image appears and disappears at specific positions along the rail, depending on the contact angle of the mercury with the mica. The optical geometry is summarized in Figure 2, and the following simple geometric argument is used to relate the contact angle to the position of the filament along the optical rail, which is easily measured.

The height of the filament *z* and the position of the knife edge defining the angle α were fixed during the experiments and measured with use of a travelling telescope. Typical values were $z = 100$ mm and $\alpha = 25°$. The lateral travel of the filament along the rail, *x*, was measured by using a ruler that was fixed on the side of the optical rail (±0.5 mm). The zero reference for *x* was taken as the point where the filament was directly above the three-phase line. Since the mica was very thin (~0.5 mm) compared to *z*, the distance *x*′ shown in Figure 2 was always very small. Ignoring it and uncertainties due to movement of the three-phase line (<0.5 mm) create negligible errors in determining the contact angle.

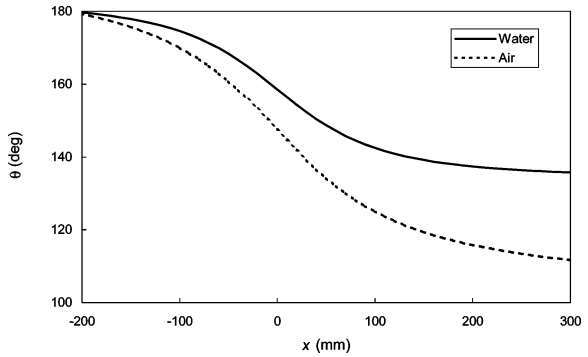

Figure 3. The relation between contact angle of the test liquid θ and the position of the filament *x* for which extinction occurs at the viewing angle α. Calculated from eq 7 with $z = 100$ mm, $\alpha = 25°$, $n_a = 1$, $n_m = 1.58$, and $n_w = 1.33$ (aqueous solution, solid line) or $n_w = 1$ (dry N_2, dashed line).

The contact angle can be related to the fixed parameters *z* and α, and the variable *x*, through Snell's law applied to the incident and reflected rays:

$$\frac{\sin\phi'_a}{\sin\phi'_m} = \frac{n_m}{n_a} = \frac{\sin\phi_a}{\sin\phi_m} \tag{3}$$

$$\frac{\sin\phi'_m}{\sin\phi'_w} = \frac{n_w}{n_m} = \frac{\sin\phi_m}{\sin\phi_w} \tag{4}$$

where n_m, n_w, and n_a are the refractive indices of mica, water, and air, respectively, and the angles ϕ are defined in Figure 2. The following relationships are derived from simple geometrical considerations:

$$\theta = \pi - \beta = \pi - \frac{1}{2}(\phi_w + \phi'_w) \tag{5}$$

$$\sin\phi_a = \sin\left(\frac{\pi}{2} - \alpha\right) = \cos\alpha \tag{6}$$

Combining eqs 3−6 and using $\sin\phi'_a = x/(x^2 + z^2)^{1/2}$ then give the desired relationship:

$$\theta = \pi - \frac{1}{2}\left[\sin^{-1}\left(\frac{\cos\alpha}{n_w}\right) + \sin^{-1}\left(\frac{x}{n_w\sqrt{x^2 + z^2}}\right)\right] \tag{7}$$

Thus, by sliding the filament along the optical rail at a fixed height *z*, and noting the minimum value of *x* just prior to extinction of the image at *I*, eq 7 yields the contact angle θ. A typical calculation is shown in Figure 3 for $z = 100$ mm and $\alpha = 25°$, when the chamber contains dry N_2 gas ($n_w = 1$) or when the mercury and substrate are immersed in a dilute electrolyte ($n_w = 1.33$). The measurement uncertainty in *x* (±0.5 mm) corresponds to an uncertainty in θ of 0.1° or less.

Note that extinction will also be observed when the ray emerging from the mercury surface is totally internally reflected at the mica/solution interface. This occurs when ϕ_m is around 39°, which is possible if the chamber is filled with electrolyte ($n_w = 1.33$, and taking the refractive index of mica $n_m = 1.58$) and the angle $\phi_w = 49°$. Each experimental configuration was checked to ensure that the critical angle did not give a "false" extinction for the angles studied. Incidentally, extinction due to total internal reflection could also have been used to measure the contact angle, but in practice this turned out to be more ambiguous due to extraneous reflections from regions of the mercury surface far from the contact point.

TABLE 1. Applied Potential E_c at Which the Electrolyte Film Separating Mercury from Mica Collapsed

electrolyte	E_c (mV)[a]	E_{ecm} (mV)[c]
0.001 M NaF	-498 ± 14[b]	-434
0.1 M NaF	-505 ± 4	-435
0.001 M KCl	-407 ± 17	-438

[a] Measured with respect to a saturated calomel electrode (SCE). [b] The uncertainty is taken as the largest deviation from the mean value since the number of samples was less than four. [c] Literature data for the electrocapillary maximum E_{ecm} from ref 31.

Materials. Electronic grade mercury (>99.9999%) was purchased from Sigma-Aldrich, and further purified with the following procedure.[24,28] Before each experiment about 100 mL of mercury was filtered through a pinhole made in Whatman filter paper into a clean Pyrex bottle. About 300 mL of 10% nitric acid was poured over the mercury and a steady stream of pure oxygen was bubbled through the two liquid layers overnight. The 10% nitric acid layer was removed by repeatedly aspirating and rinsing with distilled water until the pH of the rinse water returned was near neutral. The purified mercury was then transferred to a Teflon/glass gastight syringe (Hamilton, USA) via Teflon tubes without exposure to the atmosphere.

Potassium chloride and sodium fluoride (AR grade) were purchased from Fluka and used as received. Water was passed through a four-cartridge ion-exchange filter and distilled in an all-quartz sub-boiling still (Quartz & Silice, France) prior to use.

Results

Dry Nitrogen. The contact angle of mercury on mica was measured in dry nitrogen as a check of the system. The advancing contact angle was $128 \pm 2°$ and the receding angle was $119 \pm 2°$. Good and Paschek made similar measurements on glass and silica[10] and found that the contact angle was dependent on the state of hydroxylation of the glass and the relative humidity. The humidity in the chamber used in the present study was not measured, but should have been very low given that the purging nitrogen was filtered through a desiccant. The advancing and receding contact angles reported by Good and Paschek at their lowest humidity ($\sim$0.3) on silica were 135° and 124°, respectively, comparable to the range measured here.

Film Collapse. In aqueous solution, the mercury only came into intimate contact with the mica and partially wet it when pushed against the mica under certain conditions. When the applied potential on the mercury was sufficiently large and negative, a stable film of electrolyte prevented the mercury from wetting the mica (which is known to have a negative surface charge[29]). As the mercury potential was gradually made less negative, the film of electrolyte collapsed at a specific potential. The collapse was readily visible to the naked eye and the applied potential at which film collapse occurred, E_c, was reproducible. This behavior is consistent with the measurements of Connor and Horn[25] of aqueous film thickness between mercury and mica as a function of potential applied to the mercury phase, and similar measurements of Matsumoto and Takenaka between mercury and glass.[30] Table 1 shows the potential of film collapse and the reproducibility for different electrolyte conditions investigated. The table also compares this to the electrocapillary maximum E_{ecm} measured in previous studies under similar electrolyte conditions.[31]

After collapse of the aqueous film, the mercury partially wet the mica substrate. Note that returning the applied potential to a high negative value did not cause the aqueous film to reform at the same potential; instead the mercury remained in contact with the mica. We discuss this in the next section.

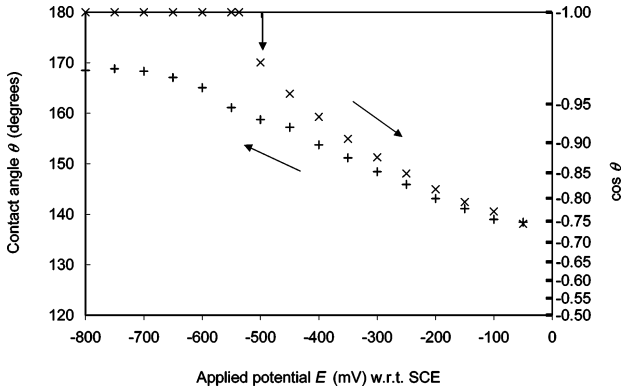

Figure 4. The contact angle θ of mercury on mica in the presence of 1 mM NaF as a function of the applied potential, for increasing potential (×) and decreasing potential (+). (NB potential is plotted in the opposite sense to the convention sometimes used in the electrochemistry literature.)

Mercury Contact Angle. After the mercury partially wet the mica surface, a decrease in the contact angle of the mercury was observed as the applied potential was moved further to the positive side of the PZC, for all electrolytes studied. Figure 4 shows the mercury contact angle for a complete cycle of applied potential in 1 mM NaF. The rupture of the aqueous film occurred at -498 mV (SCE). Continued increase of the applied potential caused the contact angle to further decrease monotonically, with a change of 0.5 V changing the contact angle by approximately 30°. Decreasing the applied potential (i.e. making it more negative) from a value higher than E_c caused the contact angle to increase, but detachment of the mercury from the mica was never observed over the potential range 0 to -1600 mV (hydrogen evolution at the mercury surface prevents the application of potentials more negative than this). Some hysteresis therefore exists between the forward and reverse directions of changing the applied potential. In common with hysteresis loops in other systems, it may be that the amount of hysteresis depends on the position of the turning point (at -50 mV in this case), but this was not explored here.

Contact angle hysteresis was also measured in the same electrolyte by the more conventional means of recording the advancing and receding angles accessed by increasing and decreasing the volume of mercury protruding from the trough at a fixed potential. Starting from the collapse point, potential was stepped up in 50-mV increments and then held fixed while the advancing and receding angles were measured. Results are shown in Figure 5, where it is seen that hysteresis is similar whether caused by changing the drop volume or the applied potential (although no measurements were made to investigate this for potentials below -500 mV). Note that in this figure $\cos\theta$ is plotted to highlight the variation in terms of interfacial energies.

Figure 6 displays data measured in 100 mM NaF with increasing and decreasing potentials and volumes, showing similar trends and hysteresis. The collapse potential is similar to that for 1 mM NaF, as one might expect from the fact that the PZC in NaF is independent of concentration,[2] but in the partial wetting regime the contact angles in 100 mM NaF are slightly higher for the corresponding values of potential.

Measurements made in 1 mM KCl with increasing and decreasing drop volumes are plotted in Figure 7. Qualitatively the behavior is the same, although as mentioned previously the collapse potential is different in this case.

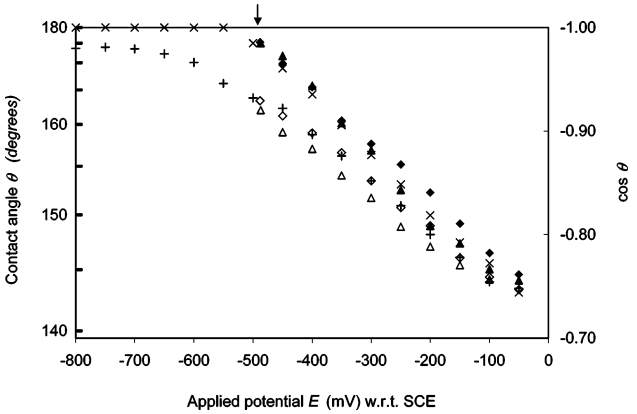

Figure 5. Cosine of the contact angle θ of mercury on mica (right-hand scale; the nonlinear scale on the left shows θ) in the presence of 1 mM NaF as a function of the applied potential. The advancing (filled symbols) and receding angles (open symbols) were obtained by increasing or decreasing the volume of mercury protruding from the mercury container and recording the maximum or minimum angle, for fixed values of applied potential. Two runs are shown, and the data from Figure 4 are included for comparison.

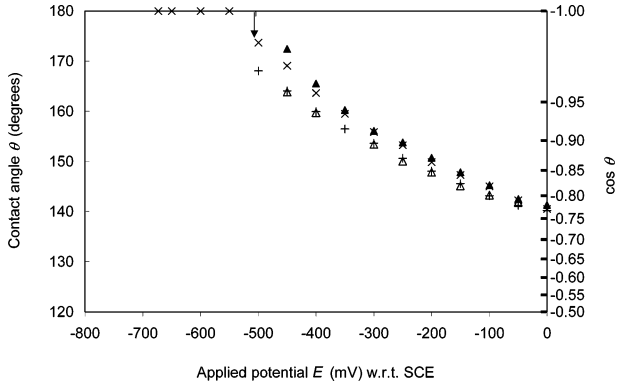

Figure 6. Contact angle θ of mercury on mica in the presence of 100 mM NaF as a function of the applied potential, measured with increasing (×) and decreasing (+) potentials, and for increasing (▲) and decreasing (△) drop volumes at fixed potentials.

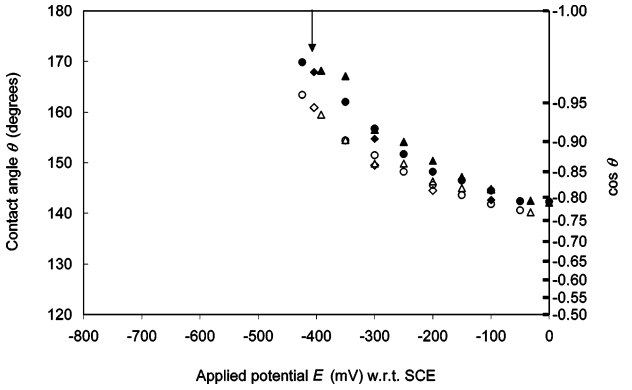

Figure 7. The contact angle θ of mercury on mica in the presence of 1 mM KCl as a function of the applied potential. The advancing (filled symbols) and receding angles (open symbols) were obtained in three separate runs (represented by different symbols) by increasing or decreasing the volume of mercury protruding from the mercury container and recording the maximum or minimum angle at fixed values of applied potential.

Discussion

The transition between a completely nonwetting mercury drop and a partially wetting drop on mica can be understood in terms of the surface forces acting between mercury and mica in the presence of electrolyte solution. When a potential that is more negative than E_{ecm} is applied to mercury, its surface becomes negatively charged in electrolyte solution, giving rise to a double-layer repulsion between it and the mica surface, which has an inherent negative charge in simple aqueous electrolytes.[29] Under these conditions there is a positive disjoining pressure that stabilizes a thin aqueous film typically some tens of nanometers thick between the mercury drop and the mica.[25] In other words, the mica is completely wet by water, and not at all by mercury. When the potential is made more positive than the collapse potential, van der Waals attraction combined with a weak double-layer repulsion or, for increasing potentials, double-layer attraction cause the mercury and mica surfaces to come into contact. Connor[24] also observed an effect similar to the hysteresis observed in Figures 4−7: that once collapsed, it was not possible to separate a mercury drop from mica by decreasing the potential again. The measured collapse potentials for KCl (Table 1) are close to the PZC and are consistent with the values reported by Connor; the values for NaF occur at potentials about 70 mV lower than the literature values for E_{ecm}. The explanation for this discrepancy may be that there were inconsistencies in the cell resistances in our experiments with different electrolytes, leading to different experimental *iR* drops in the potential.

In the partial wetting regime, analysis of the observed changes in the mercury contact angle starts with a consideration of Young's eq 1, which can be rewritten

$$\gamma_{MiAq} = \gamma_{HgMi} + \gamma_{HgAq}\cos\theta = \gamma^{0}_{HgMi} - \pi_{HgMi} + \gamma_{HgAq}\cos\theta \quad (8)$$

The subscripts identify the interfaces between phases Mi = mica, Hg = mercury, and Aq = aqueous electrolyte. For the purposes of later discussion, we have included in the second expression of this equation a "spreading pressure" term

$$\pi_{HgMi} = \gamma^{0}_{HgMi} - \gamma_{HgMi} \quad (9)$$

to account for possible differences in mercury/mica interfacial energy between a perfectly dry state (γ^{0}_{HgMi}) and in the presence of water (γ_{HgMi}).

For each of the electrolyte conditions studied, γ_{HgAq} is expected to vary with the applied potential, as shown from electrocapillary data measured in numerous studies.[2,32] Likewise in our system, γ_{HgAq} should be decreasing as the potential is increased above the PZC, which is close to E_c. If γ_{MiAq} and γ_{HgMi} were assumed to be independent of the applied potential, eq 8 would predict that θ should *increase* as the applied potential increases in this range. However, the results presented above (Figures 4−7) show the opposite behavior. Hence the observed decrease in contact angle cannot be due to the change in γ_{HgAq} alone, and evidently γ_{MiAq} and/or γ_{HgMi} must also be varying with the applied potential.

Since mica is an insulator there seems no reason to suppose that any change to γ_{MiAq} occurs when a potential is applied between mercury and the aqueous phase, even when the mica contacts both. The value of γ_{MiAq} is known from measurements of adhesion between two mica surfaces immersed in electrolyte solution in the SFA. A typical value for dilute solutions is 10 mJ/m,[2,33] much smaller than γ_{HgAq}, and not strongly dependent on electrolyte type. Repulsive hydration forces prevent adhesion between mica surfaces at electrolyte concentrations above 0.1 mM in KCl and 10 mM in NaCl,[34] so we set $\gamma_{MiAq} = 0$ in analyzing the 1 mM KCl and the 100 mM NaF data. Taking

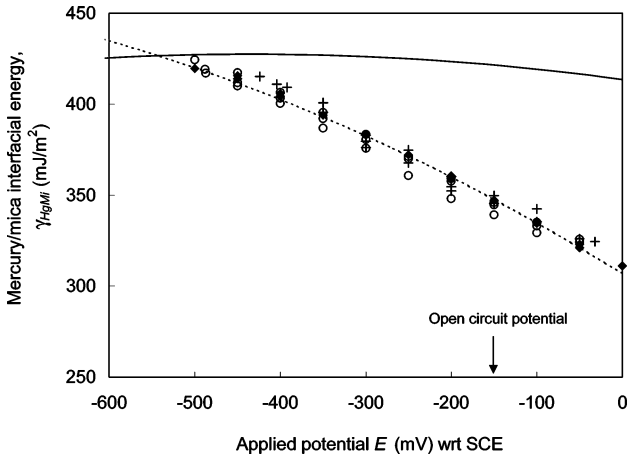

Figure 8. Variation with applied potential of the mercury/mica interfacial energy derived from Young's eq 1, using literature data for γ_{MiAq} and γ_{HgAq}, and the data of Figures 4−7 for the average contact angles measured in 1 mM NaF (○), 100 mM NaF (◆), and 1 mM KCl (+). The solid curve is the variation of mercury/aqueous interfacial tension in 1 mM NaF,[35] and the dotted line is a fit to the 100 mM NaF data, using the estimated value of capacitance between mica and mercury (see Discussion).

these values together with literature data for γ_{HgAq}[35] and the measured contact angles from Figures 4−7 (using the average of cosθ advancing and receding) as a function of applied potential allows the mica/mercury interfacial tension γ_{HgMi} to be determined. The results are plotted in Figure 8, from which it is seen that γ_{HgMi} varies significantly with changes in the potential applied to mercury with respect to a reference electrode in the aqueous phase.

A simple explanation for why γ_{HgMi} should be a function of applied potential has the same basis as electrocapillarity of the mercury/aqueous interface, namely that the mica/mercury interface is also charged. In that case, the interfacial energy varies with potential according to the Lippmann equation (eq 2), where in this instance $\gamma = \gamma_{HgMi}$, and $\sigma = \sigma_{HgMi}$ is the charge per unit area on the mercury surface at its interface with mica. To apply this equation we must assume that the Galvani potential of mica is unaffected by the potential E applied between electrodes in the mercury and aqueous phases. This would be the situation if both the mercury/aqueous and mercury/mica interfaces are perfectly polarizing, i.e. that no current crosses these interfaces. That is well-known[2,3] to be the case for mercury/aqueous electrolyte over the range of potentials explored in these experiments, and it is also reasonable to suppose that no current passes to or from mica, which is an excellent insulator. Under these conditions, eq 2 allows the surface charge σ_{HgMi} to be calculated from the gradient of the data in Figure 8. This gives $\sigma_{HgMi} = +0.26$ C/m^2, ascertained from the gradient of the dotted line (which will be discussed later) at the open circuit potential, i.e., the natural potential difference existing between the connecting electrodes when no external potential is applied. This was measured as −150 mV SCE.

This result shows that mercury tends to adopt a positive charge at its interface with mica at the open circuit potential. The conclusion is consistent with past observations that mica is charged negatively in contact with simple electrolyte solutions, while mercury is charged positively in these solutions in the absence of applied potential. Under these conditions, strong double-layer attraction has been observed between mercury and mica in KCl solutions.[24,25,36] Positive charging of mercury in contact with mica is presumably also the situation that would pertain in the absence of water, and hence contact electrification experiments would be expected to show mercury charging positively and mica negatively. Indeed, although there is some confusion in the literature attributable to contamination of mercury by oxide films in some experiments,[37] clean mercury does occupy a higher (more positive) position than mica in the triboelectric series, which is consistent with the present finding.[38] Observations of triboelectric phenomena with mercury against glass or silica[5,39,40] also show mercury charging positively in contact with these materials.

The mechanism of charge transfer across interfaces involving insulating materials is not known in general. Possibilities include transfer of electrons, ions, or fragments of material.[37,41] For mercury/mica, ion transfer provides a possible explanation, as discussed below. However, we emphasize that our results do not provide proof of this mechanism, and also that its correctness or otherwise is not important for the remainder of our discussion. When mica contacts water it is known that some of the surface potassium ions, which compensate negative lattice charge in the mica crystal, dissolve in the water and leave a net negative charge on the mica.[34] A simple possibility in the mercury/mica contact is that potassium ions are likewise dissolved in mercury (which is well-known to dissolve most metals), thereby charging the mercury positively and the mica negatively. The number of potassium ions per unit area of mica surface is known (2.28×10^{18} m^{-2}); if all of them were removed the mica surface charge would be 0.343 C/m^2.[42] Thus the value for charge density obtained from the slope of Figure 8 (0.26 C/m^2) is consistent with about 75% of the available potassium ions from a mica surface entering the mercury and transferring their charge to that phase. (We note however that this mechanism would not be relevant for contact electrification between mercury and glass, which produces the same charging polarity.) Since mercury is a good conductor, all of its charge must reside at the surface. However, it would not necessarily spread uniformly over the entire mercury surface, since electrostatic attraction would hold much of it close to the negative sites just beneath the mica surface. As we discuss below, the charge distribution will depend on the relative capacitances between mercury and its neighboring materials.

It should be noted that the inherent interfacial charge density established from this analysis is much higher than what would be measured in a conventional contact electrification experiment, in which charges are measured only after separation of two materials. In such experiments, tunneling and/or gas discharge enable most surface charge to return to its original material during the initial stages of separation, and only a much lower residual charge can be measured.[41,43,44]

Previous authors[6−11] have offered a different explanation for the variation of interfacial energy between mercury and various insulating materials (including gases) in terms of the spreading pressure (eq 8). For example, Gorodetskaya et al.[6] and Nakamura et al.[8] explain their data by supposing that π_{HgMi} is a function of potential.

The spreading pressure introduced in eq 8 can be written as

$$\pi_{HgMi} = \int_0^{h_0} \Pi_{HgMi}(h)\, dh = V_{HgMi}(0) - V_{HgMi}(h_0) \qquad (10)$$

in which $\Pi_{HgMi}(h)$ is the disjoining pressure in an aqueous film of thickness h between flat mica and mercury surfaces, which is the same as the force per unit area acting between these surfaces, and $V_{HgMi}(h)$ is the interaction free energy per unit area in this configuration. The spreading pressure would be

nonzero if a finite thickness h_0 of aqueous phase remained between mercury and mica after they collapse into "contact". This could occur if there were a repulsive hydration force between them due to a hydration layer on one or both surfaces, which could hold them apart against the van der Waals attraction that would otherwise pull them together.

There are no measurements of hydration forces in this system. From optical interferometric measurements of mercury/mica separation between mica and positively charged mercury[24] we have not detected any hydration layer, and if it existed we can place an upper limit on its thickness of 1 nm. If a hydration force were present, a reasonable estimate of its magnitude and range would be to use the data of Pashley,[34] who measured mica−mica hydration forces and found

$$V_{\mathrm{MiMi}}^{\mathrm{hyd}} = V_0 \exp\{-h/\lambda\} \tag{11}$$

with $\lambda \approx 0.3$ to 0.9 nm and V_0 between 3 and 20 mJ/m^2 for simple monovalent electrolytes. Using the largest of these values with the shortest decay length, and the experimental upper limit for h_0 of 1 nm, would give an upper bound for π_{HgMi} of 20 mJ/m^2. The *change* in γ_{HgMi} seen in Figure 8 is considerably more than this, from which we conclude that a spreading pressure term alone cannot account for the observed variation of mica/mercury interfacial energy with potential.

Furthermore, the hydration of mica is known to be dramatically different between Na^+ and K^+ electrolytes at a concentration of 1 mM.[34] Our results show similar dependence of γ_{HgMi} on potential for 1 mM NaF and KCl solutions, so we do not believe that invoking a variable spreading pressure provides the correct explanation for the observed contact angle variation. The charged-interface model that we propose is simple and it is consistent with the observations. We note that although Nakamura et al.[8] discussed their results in terms of a variable spreading pressure, they also calculated a charge density at the mercury/air interface in the same way as we have done here (implicitly making use of the Lippmann equation), and their calculated charge behaves qualitatively in the same way as the mercury charge at the aqueous interface. This would be expected of a metallic conductor, for which charges at a free surface must be proportional to the charges existing at another region of the surface to maintain a uniform electrical potential throughout the conductor.

Finally, returning to our own experiment, we note that electrical conductivity ensures the charge densities on the regions of the mercury surface contacting the solid and electrolyte phases are not independent of each other. If charge is altered at one part of the mercury surface (e.g. where it is in contact with aqueous electrolyte) then the charge at another part of the surface will also be affected. The change in surface charge densities σ_i at the two mercury interfaces in response to applied potential will be related by the ratio of differential capacitances C_i at the two interfaces:

$$\frac{\partial \sigma_{\mathrm{HgMi}}}{\partial \sigma_{\mathrm{HgAq}}} = \frac{\partial \sigma_{\mathrm{HgMi}}}{\partial E}\,\frac{\partial E}{\partial \sigma_{\mathrm{HgAq}}} = \frac{C_{\mathrm{HgMi}}}{C_{\mathrm{HgAq}}} \tag{12}$$

A first estimate of capacitance at the mercury/mica interface can be obtained by considering the charge to lie in two planes, one on the mercury surface and the other being the inherent negative lattice charge of mica, generally thought to reside on aluminum ions at tetrahedral sites situated at a depth d_t below the surface of mica's aluminosilicate sheets.[45] In this approximate picture, the differential capacitance per unit area is $C_{\mathrm{HgMi}} = \epsilon_0\epsilon_{\mathrm{Mi}}/d_t$. Taking $\epsilon_{\mathrm{Mi}} \approx 6$ and estimating $d_t \approx 0.2$ nm (P. G. Slade, personal communication) gives $C_{\mathrm{HgMi}} \approx 0.3$ F/m^2. Since $C_{\mathrm{HgMi}} = \partial\sigma_{\mathrm{HgMi}}/\partial E = -\partial^2\gamma_{\mathrm{HgMi}}/\partial E^2$, this estimate of capacitance has been used to fix the curvature of the dotted line in Figure 8. This provides a reasonable fit to the data for 100 mM NaF, but the other data sets appear to follow straighter lines, so the actual capacitance may be smaller than our crude estimate.

Differential capacitance per unit area at the mercury/aqueous phase is available from the classical electrochemistry literature;[32] for 1 mM NaF a typical value in the neighborhood of the PZC is $C_{\mathrm{HgAq}} \sim 0.1$ F/m^2.[2] Hence, from eq 12, the variation with polarizing potential of the charge at the mercury/mica interface is a few times greater than the variation at the mercury/electrolyte interface. However, the *magnitude* of charge at the mercury/mica interface is significantly higher than σ_{HgAq} over the range of potentials covered here. In particular, at the open circuit potential, the mercury charge density at its mica interface is estimated as +0.26 C/m^2 compared with literature values of +0.05 C/m^2 on mercury in contact with 1 mM NaF, or 0.08 C/m^2 in 100 mM NaF.[46]

According to this discussion, surface charge of mercury (or any other conductor) at its interface with one material, e.g. water, is not independent of its surface charge where it contacts another, mica in this case. However, it is beyond the scope of this article to explore further the question of whether this affects the universality of surface charge results derived, for example, from electrocapillary or dropping mercury electrode experiments.

The sensitivity of contact angle to applied potential that we have demonstrated here is much greater than recent electrowetting experiments in which potential is applied between an aqueous phase and an electrode behind an insulating substrate.[15,20,22] In those experiments, typical results show a change in contact angle of a few tens of degrees when a potential of a few hundred volts is applied, compared to a similar change measured here in response to a few hundred millivolts. The reason is simply related to the high inherent charge density at the mercury interfaces, as can be seen from the following analysis. The variation of contact angle with potential can be specified by an "electrowetting coefficient":

$$\frac{\partial \cos\theta}{\partial E} = \frac{\partial}{\partial E}\left(\frac{\gamma_{13} - \gamma_{12}}{\gamma_{23}}\right) \tag{13}$$

which after a little algebra can be written as

$$\frac{\partial \cos\theta}{\partial E} = \frac{1}{\gamma_{23}}\frac{\partial}{\partial E}\{\gamma_{13} - \gamma_{12} - \gamma_{23}\cos\theta\} \tag{14}$$

If one or more of the interfaces is charged, and polarizable by the applied potential E, then use of the Lippmann eq 2 gives:

$$\frac{\partial \cos\theta}{\partial E} = \frac{1}{\gamma_{23}}\{\sigma_{12} - \sigma_{13} + \sigma_{23}\cos\theta\} \tag{15}$$

In the present case the applied potential polarizes *two* interfaces, mercury/aqueous and mercury/mica, so that two (the first and third) of the terms inside the brackets in eq 15 are nonzero. The analysis shows that change in contact angle is determined primarily by the interface with the highest surface charge, which is mercury/mica.

The charge on an interface could be an inherent property of the two materials, as in the present experiments, or it could be induced by application of an electric field across an insulator, as in the water-drop electrowetting experiments.[15,20,22] For an induced charge, a slightly different analysis of the capacitive

contribution to interfacial energy leads to a formally similar result with surface charge of the solid given by $\sigma_{12} = C_f E$, where $C_f = \epsilon_f \epsilon_0 / d_f$ is the capacitance per unit area of the insulating film of dielectric constant ϵ_f and thickness d_f.[20] Other surface charges are not considered because the interfaces are not polarized by the applied potential in those experiments. The capacitance available across a micron-scale insulating film is typically ca. $1-10\ \mu F/m^2$, and potentials of ca. 100 V induce surface charges that are still 2−3 orders of magnitude less than the naturally occurring charges at the mercury interfaces.

Conclusion

We have measured the contact angle of a mercury drop immersed in aqueous electrolyte solution when it makes contact with a flat mica surface. With an electrical potential applied between the mercury and aqueous phases, the mercury partially wets the mica over a certain range of potential, and its contact angle varies as the potential is varied. The change in contact angle cannot be accounted for by considering only the well-known dependence of mercury/aqueous interfacial energy on applied potential. However, it can be explained if the mercury/mica interface is charged, so that the energy of that interface also becomes a function of the potential of the mercury phase. Variation in spreading pressure, which has been proposed by previous authors for other systems involving mercury, is not able to explain the observed behavior.

The gradient of the potential variation of interfacial energy allows us to estimate the surface charge density of mercury in contact with mica. This charge density is several times higher than typical charges at the mercury/electrolyte interface. We attribute this to natural contact electrification between the mercury and mica, and note that the sign of the charge is consistent with other contact charging measurements. A plausible mechanism for charging at this interface is suggested, namely that potassium ions from the mica surface can dissolve in the mercury, leaving an uncompensated negative lattice charge in the mica. However, this mechanism (which is not essential for the other parts of our discussion) would not be applicable to the mercury/glass combination for which comparable charging behavior has been observed.

The contact angle changes because interfacial energy is sensitive to potential, not at one but at two of the interfaces between the three phases. Charge density at the two interfaces is coupled because the mercury is a good conductor and must therefore maintain an equipotential throughout. Our results suggest that care should be taken in analyzing other systems, such as capillary rise measurements with mercury in contact with an aqueous phase, or the abovementioned electrowetting measurements with aqueous drops, if there is any possible mechanism for coupling potential-determining charged species in one of the phases. In particular, as previously suggested by Lawrence et al.,[4] the contact angle of mercury in a capillary cannot be assumed to be constant in electrocapillarity measurements.

What we have observed is a particular form of electrowetting, in which contact angle is modified by an applied potential. The high inherent surface charge densities present at mercury interfaces mean that the potentials required to effect significant contact angle changes in this system are of much smaller magnitude than those required to alter the contact angle of an aqueous phase contacting an insulating film.

Acknowledgment. This work was funded by the Australian Research Council. The authors would like to thank several people with whom we have had useful discussions concerning this work: Wuge Briscoe, Hugo Christenson, Tom Healy, Karl-Heinz Muller, Ric Pashley, Brian Pethica, Jordon Petrov, and Phil Slade.

References and Notes

(1) Smolders, C. A. *Recl. Trav. Chim. Pays-Bas* **1961**, *80*, 650.
(2) Grahame, D. C. *Chem. Rev.* **1947**, *41*, 441.
(3) Hunter, R. J. *Foundations of Colloid Science*, 2nd ed.; Oxford University Press: Oxford, UK, 2001.
(4) Lawrence, J.; Parsons, R.; Payne, R. *J. Electroanal. Chem.* **1968**, *16*, 193.
(5) Kolthoff, I. M.; Kahan, G. J. *J. Am. Chem. Soc.* **1942**, *64*, 2553.
(6) Gorodetskaya, A. V.; Frumkin, A. N.; Titievskaya, A. S. *Zh. Fiz. Khim.* **1947**, *21*, 675.
(7) Smolders, C. A. *Recl. Trav. Chim. Pays-Bas* **1961**, *80*, 699.
(8) Nakamura, Y.; Kamada, K.; Katoh, Y.; Watanabe, A. *J. Colloid Interface Sci.* **1973**, *44*, 517.
(9) Ivosevic, N.; Zutic, V. *Langmuir* **1998**, *14*, 231.
(10) Good, R. J.; Paschek, J. K. The Wetting of Outgassed Glass and Silica by Mercury, and the Dependence of the Contact Angle on Water Vapour Pressure. In *Wetting, Spreading, and Adhesion*; Padday, J. F., Ed.; Academic Press: London, UK, 1978; p 147.
(11) Xu, Z.; Liu, Q.; Ling, J.; Summer, A. *Langmuir* **1996**, *12*, 547.
(12) Colgate, E.; Matsumoto, H. *J. Vac. Sci. Technol., A* **1990**, *8*, 3625.
(13) Prins, M. W. J.; Welters, W. J. J.; Weekamp, J. W. *Science* **2001**, *291*, 277.
(14) Berge, B.; Peseux, J. *Eur. Phys. J. B* **2000**, *3*, 159.
(15) Quinn, A.; Sedev, R.; Ralston, J. *J. Phys. Chem. B* **2003**, *107*, 1163.
(16) Murphy, O. J.; Wainwright, J. S. *Langmuir* **1989**, *5*, 519.
(17) Hato, M. *J. Colloid Interface Sci.* **1989**, *130*, 130.
(18) Perng, Y.-Y.; Lichter, S. *J. Colloid Interface Sci.* **1999**, *217*, 119.
(19) Sondag-Huethorst, J. A. M.; Fokkink, L. G. J. *Langmuir* **1992**, *8*, 2560.
(20) Vallet, M.; Berge, B.; Vovelle, L. *Polymer* **1996**, *37*, 2465.
(21) Welters, W. J. J.; Fokkink, L. G. J. *Langmuir* **1998**, *14*, 1535.
(22) Peykov, V.; Quinn, A.; Ralston, J. *Colloid Polym. Sci.* **2000**, *278*, 789.
(23) Janocha, B.; Bauser, H.; Oehr, C.; Brunner, H.; Gopel, W. *Langmuir* **2000**, *16*, 3349.
(24) Connor, J. N. Measurement of Interactions between Solid and Fluid Surfaces, Ph.D. Thesis, University of South Australia, 2001.
(25) Connor, J. N.; Horn, R. G. *Langmuir* **2001**, *17*, 7194.
(26) Langmuir, I.; Schaeffer, V. J. *J. Am. Chem. Soc.* **1937**, *59*, 2405.
(27) Fort, T.; Patterson, H. T. *J. Colloid Interface Sci.* **1963**, *18*, 217.
(28) Gordon, C. L.; Wichers, E. *Ann. N. Y. Acad. Sci.* **1957**, *65*, 369.
(29) Lyons, J. S.; Furlong, D. N.; Healy, T. W. *Aust. J. Chem.* **1981**, *34*, 1177.
(30) Matsumoto, M.; Takenaka, T. *Bull. Inst. Chem. Res. Kyoto Univ.* **1982**, *60*, 269.
(31) Conway, B. E. Properties of the Electric Double Layer at Interfaces. In *Electrochemical Data*; Elsevier Publishing Company: Amsterdam, The Netherlands, 1952; p 215.
(32) Lyklema, J.; Parsons, R. Electrical properties of interfaces—compilation of data on the electrical double layer on mercury electrodes, U.S. National Bureau of Standards Internal Report 83-2714, 1983.
(33) Christenson, H. K. *J. Colloid Interface Sci.* **1988**, *121*, 170.
(34) Pashley, R. M. *J. Colloid Interface Sci.* **1981**, *83*, 531.
(35) Coung, N. H.; D'Alkaine, C. V.; Jenard, A.; Hurwitz, H. D. *J. Electroanal. Chem.* **1974**, *51*, 377.
(36) Horn, R. G.; Bachmann, D. J.; Connor, J. N.; Miklavcic, S. J. *J. Phys.: Condens. Matter* **1996**, *8*, 9483.
(37) Harper, W. R. *Contact and Frictional Electrification*; Oxford University Press: Oxford, UK, 1967.
(38) Shaw, P. E. *Proc. R. Soc. London, A* **1918**, *94*, 16.
(39) Yaminsky, V. V.; Johnston, M. B. *Langmuir* **1995**, *11*, 4153.
(40) Budakian, R.; Weninger, K.; Hiller, R. A.; Putterman, S. J. *Nature* **1998**, *391*, 266.
(41) Lowell, J.; Rose-Innes, A. C. *Adv.. Phys.* **1980**, *29*, 947.
(42) Quirk, J. P. *Adv. Agron.* **1994**, *53*.
(43) Montgomery, D. J. Static Electrification of Solids. In *Solid State Physics. Advances in Research and Applications*; Seitz, F., Turnbull, D., Eds.; Academic Press: New York, 1959; Vol. 9, p 139.
(44) Horn, R. G.; Smith, D. T. *Science* **1992**, *256*, 362.
(45) Schultz, P. K.; Slade, P. G.; Tiekink, E. R. T. *N. Jb. Miner. Mh.* **1989**, *3*, 121.
(46) Grahame, D. C. *J. Am. Chem. Soc.* **1954**, *76*, 4819.